JTTEE5 12:403-415

Particle Temperature and Velocity Effects on the Porosity and Oxidation of an HVOF Corrosion-Control Coating

T.C. Hanson and G.S. Settles

(Submitted 15 October 2001; in revised form 4 September 2002)

Independent control of particle velocity and temperature in the HVOF process has been achieved in this research, allowing these variables to change by 170 m/s and 200 °C, respectively. The independence was achieved using a specially designed nozzle with multiple powder injection ports and by an inert diluent added to the oxygen stream feeding the combustion. Within the available range, notable changes in splat morphology, porosity, and coating oxidation of sprayed 316L stainless steel are readily apparent. Increased particle velocity generally correlates with improved splat deformation but has a weak effect on porosity and no effect on oxidation. Particle temperature, on the other hand, correlates strongly with highly deformed splats, porosity, and oxidation. In fact, highly dense coatings having little oxidation can be formed with relatively low velocity particles if the average particle temperature is kept in the vicinity of the material melting point. This result suggests that particle temperature control is the key to creating dense, low-oxide HVOF-sprayed corrosion-control coatings. Because commercial HVOF equipment currently lacks this capability, the research indicates a useful direction for future development.

Keywords coating porosity, corrosion-control coatings, HVOF, metallography, particle diagnostics, splats

1. Introduction

Above all other variables, particle velocity and temperature are the most significant in determining the properties of a thermal spray coating. Various attempts have been made to determine the separate effects of these variables on HVOF-sprayed coating properties. While a number of methods were demonstrated to provide independence, at least over a limited range, no parametric study of the effects of such control has ever been performed over significant ranges of velocity and temperature. Here we present such a study, using 316L stainless steel as an example of a corrosion-control coating.

2. Review of Literature

Several studies began to provide some understanding of the separate effects of particle velocity and temperature on coating properties. Using a particle dynamics computer code, Hackett predicted and later demonstrated experimentally that particle velocity is primarily a function of HVOF combustion chamber pressure, while particle temperature is mainly affected by the residence time of a particle within the nozzle.[1] These experiments demonstrated independence over only small ranges of temperature and velocity but, nonetheless, showed that particle oxidation is strongly affected by the fraction of particles molten upon impact.

Voggenreiter et al. also controlled particle temperature and velocity independently, to an extent, by varying combustion pressure and the air-fuel ratio.[2,3] They, too, concluded that oxidation corresponds closely to the fraction of molten phase present in the coating. A key result of their research was the suggestion that optimum HVOF spraying occurs when the powder temperature is between the solidus and liquidus temperatures of the sprayed material.

More recently, Dobler et al. likewise showed that particle temperature is the key parameter in coating oxidation.[4] In fact, splat oxidation surprisingly decreased when the HVOF combustion mixture was oxygen-rich, since this reduced the combustion temperature and, consequently, the particle temperature. Further, they found that coating hardness correlated with particle deformation and that bond strength was poorest at the lowest particle temperatures.

In a recent paper by Sturgeon and Buxton, coatings with oxide levels of 2% by weight fared better than lower-oxide coatings in corrosive environments.[5] This is counterintuitive in principle, since higher oxides are expected to occupy greater internal surface area in a coating, thus to be more corrosion-prone. However, Sturgeon and Buxton suggested that the reason for their observation is because the low particle temperatures associated with low-oxide coatings impair the adhesion of the splats to the substrate and to one another, and also cause porosity (coatings with porosity levels above 4% are much more susceptible to corrosion).[5]

Thus, higher oxide content is an undesirable byproduct of hotter particles in HVOF coatings, in which independent spray parameter control is lacking. In fact, both of the just-cited studies used equipment that had no facility for independent control of particle temperature and velocity.[4,5] Therefore, they indicate a

T.C. Hanson and **G.S. Settles,** Pennsylvania State University, Department of Mechanical and Nuclear Engineering, University Park, PA 16802. Contact e-mail: gss2@psu.edu.

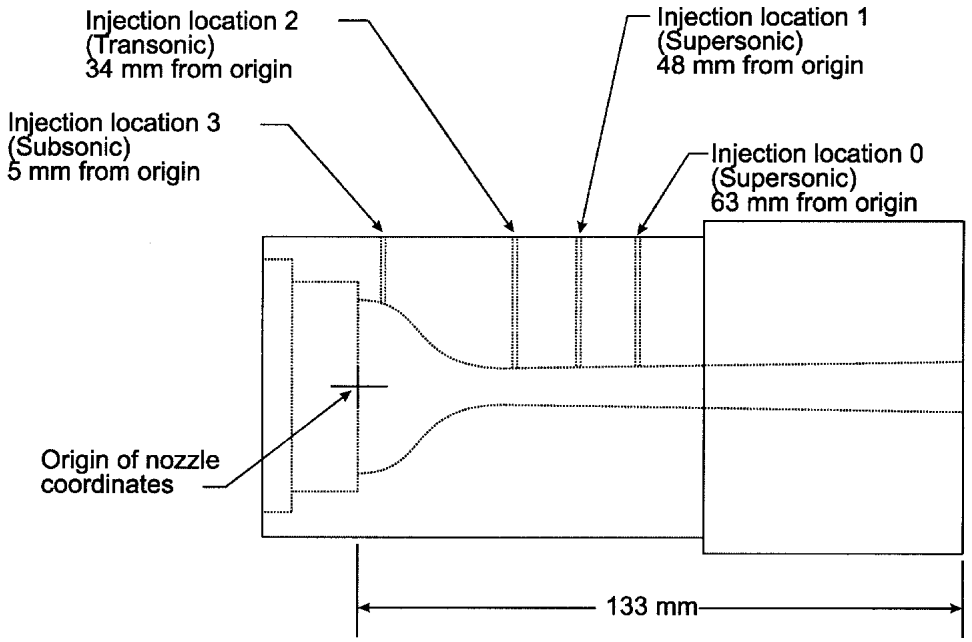

Fig. 1 Schematic diagram of the conical converging-diverging nozzle used in this study

correlation but not an explicit cause-and-effect relationship between particle oxidation and improved coating corrosion performance.

Previous HVOF research by Hanson et al. was also performed to better understand temperature and velocity effects by separating them, but the comparisons were constrained to relatively small parameter ranges.[6] Here we broaden those ranges substantially.

Recently the cold-spray process has gained attention alongside HVOF, mainly for cold-spray's promise of yielding dense coatings with exceptionally low oxidation levels. The earliest work, Alkhimov et al. (1990), established the existence of what was termed a "critical velocity."[7] When spray particles exceeded this velocity, deposition efficiency rose markedly, but so did coating porosity. In papers by McCune et al.[8] and Dykhuizen and Smith,[9] micrographs of cold-sprayed coating cross-sections are shown that are remarkably similar to those of HVOF coatings in the above-cited work where particle temperatures are kept below the melting point of the material. This suggests that careful control of HVOF spray particle parameters, if available, might provide coatings with desirable properties similar to those of cold-sprayed coatings.

2.1 Scope of Experiments

The present work is intended to elucidate the effects of independent changes in temperature and velocity of HVOF-sprayed 316L stainless steel powder particles on splat morphology, coating porosity, and coating oxidation. The need for a parametric study of the effects of these variables arises to define "ideal" spray conditions for such a corrosion-control coating. Many different settings of the HVOF torch parameters are possible, leading to a broad range of coating characteristics that are not all useful for corrosion control. This paper aims to provide direction in the choice of the proper parameters.

3. Experimental Equipment and Methods

3.1 HVOF Spray Equipment

The equipment used in these experiments has been previously described in detail [6]; therefore only the features most pertinent to the present research are discussed here. The spray torch is a modified Praxair-Tafa JP-5000 unit (Praxair-Tafa, Concord, NH) in which the original nozzle has been replaced with a conical converging-diverging Laval nozzle incorporating several axial port locations for spray particle injection. A schematic of this nozzle is given in Fig. 1. It has an 8 mm diameter throat and an 11 mm diameter exit, and it produces approximately Mach 2 flow at the exit. Nozzle locations denoted 0, 1, 2, and 3 are defined in the Fig. 1. Locations 0 and 1 are in the diverging (supersonic) section of the nozzle, while location 2 is effectively at the nozzle throat, and location 3, not used in this study, is well upstream of the throat in the subsonic nozzle region. The choice among these injection ports provides a key means to control particle temperature, as discussed in Ref. 6 and elaborated further below.

3.2 Particle Velocity and Temperature Measurements

Particle velocities were measured by streak velocimetry, while particle temperatures were measured with an Inflight 2010 two-color pyrometer (Inflight Inc., Idaho Falls, ID). Experimental accuracies were typically ±30 m/s and ±70 °C, respectively. Details of the experimental arrangement for these measurements are given in Ref. 6.

3.3 Fuel and Oxidizer

The JP-5000 HVOF torch is designed to burn liquid kerosene fuel with oxygen gas. Though Voggenreiter et al.[2,3] and Dobler

et al.[4] varied their fuel-air mixtures to control particle temperature, stoichiometric fuel-air mixtures were maintained throughout the present experiments. Instead, it was recognized early in the present research (based on the suggestion of Browning and others) that diluted oxidizer gas mixtures can provide some control of combustion temperature, and hence of particle temperature. Since our interest lies mainly in particle temperatures below the material melting point, the oxygen for combustion was diluted with nitrogen in most present experiments to lower the combustion temperature. Given our selection of a constant (stoichiometric) fuel-air ratio, adding nitrogen diluent to the oxidizer provided a means to keep particle temperatures low while maintaining high combustion pressures. A set of working charts and a calibrated pressure gauge allowed nitrogen to be added to the compressed oxygen stream in known, repeatable proportions. Thus, as much as 30% by weight of the oxidizer gas fed to the HVOF torch consisted of nitrogen diluent in these experiments.

3.4 Choice of Spray Particles

The powder sprayed in these experiments was gas-atomized 316L stainless steel powder (Praxair-Tafa, Concord, NH, #1236F). The powder particles have an average diameter of 39 μm and a standard deviation of 9 μm. This material was chosen due to its common use in corrosion-protection applications, and for comparison with previous work.[1,2,4,6]

3.5 Formation of Coatings

Coatings in these experiments were sprayed onto aluminum substrates positioned 40 cm downstream of the HVOF nozzle exit. The flowrate of powder into the torch was 70 g/min under all circumstances. Coatings were formed by passing the substrate through the particle-laden stream four to eight times at a traverse speed of approximately 10 cm/s. The metallographic preparation of these coatings involved standard sectioning, mounting, polishing, and etching procedures. An electrolytic etch was performed in a 10% oxalic acid solution, which served to render visible the splat boundaries, grain boundaries, and oxidized regions of the coating prior to micrography.

3.6 Splat Morphology and Porosity Analysis

These experiments rely heavily upon coating metallography to reveal the effects of variations in spray particle temperature and velocity. In general, at least three high-magnification (500×) microscopic images of each prepared cross-section were taken at different locations within the coating to ensure a representative sample for qualitative analysis of splat morphology, splat deformation, and oxidation. Low-magnification images (100×) were also taken to reveal larger cross-sections of the coating for porosity analysis. The coating porosity was measured using the Delesse principle [10]: if the porosity is randomly distributed throughout the coating (as we assume), then the percentage of porous area in a coating cross-section is identical to the percentage of porous volume in the entire coating.

3.7 Coating Oxygen Content Analysis

Several coatings were debonded from their substrates for oxygen content analysis (Leco RO-416DR Oxygen Determinator, Leco Corp., St. Joseph, MI). This yielded an independent quantitative measure of the coating oxidation level. The accuracy of the Leco measurements was not high (±0.5% of oxygen content by weight), but they were repeatable to within 3% of the mean in all cases.

4. Results

4.1 Particle Injection Pressure

The pressure of the carrier gas used to inject particles into an HVOF nozzle is a variable that has received little consideration in previous research. We found, however, that this pressure can have a marked effect on both particle velocity and particle temperature. The effect arises from the transverse momentum of particles injected normal to the gas stream through nozzle-wall orifices. Inadequate or excessive injection pressures can force the spray particles into the nozzle wall boundary layer, where they attain lower temperatures and velocities than do particles on the nozzle centerline. Prior to its discovery, this uncontrolled variable wreaked havoc with the experimental results. To control it, the particle injection pressure in the present experiments was adjusted for each running condition to ensure that the visibly luminous particles exited along the nozzle centerline, not the sidewalls.[12]

4.2 Particle Temperature Control

The separation of particle velocity and temperature achieved in this research builds directly on work described previously, in which it was established that particle temperature depends strongly upon the particle residence time within the nozzle.[6] Consequently, particle temperature can be affected by selecting the particle injection location along the nozzle length. Combustion pressure also affects particle temperature, however, and this diminishes the effectiveness of using only injection location and combustion pressure to separate particle velocity from particle temperature. Thus, additional control over particle temperature was gained here by adding an inert diluent (nitrogen) to the combustion gas to lower the combustion-chamber temperature while maintaining combustion-chamber pressure.

The correlations between temperature and velocity, respectively, with HVOF chamber pressure provide a clear way to understand how parameter independence was achieved in this research. The experimental measurements of particle temperature plotted against combustion chamber pressure are shown in Fig. 2. By observing the rising trend in temperature as combustion pressure increases for a fixed injection location and combustion gas mixture, one concludes the relationship is roughly linear.

This is consistent with results reported in Hackett,[1] previous measurements made by the present authors,[6] and trends predicted using a particle dynamics code.[1] Since residence time within the nozzle is mainly a function of injection location, the effect of residence time on particle temperature can be observed in Fig. 2 through comparison of the respective temperatures of particles injected at locations 0 and 1 for the 90/10 gas mixture (90% oxygen/10% nitrogen). For each pressure, particles injected at location 1 have higher temperatures than particles injected at location 0, as expected, since location 1 is upstream of location 0.

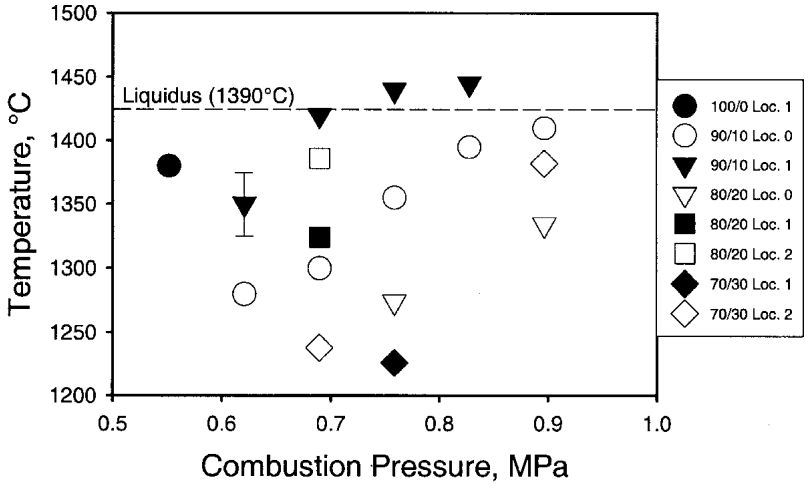

Fig. 2 Relationship between particle temperature and combustion chamber pressure. Legend: 90/10 Location 1, for example, refers to a 90% oxygen, 10% nitrogen combustion gas mixture, and particles injected at location 1 (Fig. 1). The error bar shown is indicative of the total uncertainty of temperature for the range of particle temperatures plotted, while the symbol width is indicative of the uncertainty in combustion pressure.

Combustion temperature decreases dramatically as the amount of nitrogen diluent gas increases for a fixed combustion pressure, and therefore particle temperatures for a given injection location decrease correspondingly. By observing the temperatures of particles injected at location 1 for the 100/0%, 90/10%, and 70/30% oxygen/nitrogen gas mixtures in Fig. 2, the trend of temperature reduction despite increased combustion chamber pressure indicates that dilution is an effective means to control particle temperature. The combined effects of changing particle injection location and combustion oxidizer dilution are sufficient to vary particle temperature over approximately a 200 °C range.

4.3 Particle Velocity Control

The relation between particle velocity V_p and combustion pressure is shown in Fig. 3. Clearly, particle velocity is primarily affected by combustion pressure and increases almost linearly with it. Compared with particle temperature T_p, V_p is relatively unaffected by nozzle injection location or oxidizer-gas dilution. Particles do tend to have slightly higher velocities, though, as their residence time within the nozzle increases. This effect is approximately 15 m/s in V_p per centimeter of change in injection location. Again, these trends were also observed in computations using a particle dynamics code. The error bar shown in Fig. 3 is ±30 m/s, indicating the precision error in the measurement.

4.4 Demonstration of Independent Control

Because particle velocities in this experiment remain relatively unaffected by the variables that change particle temperature, a wide range of conditions can be explored in particle temperature-velocity space. More specifically, combustion chamber pressure alters both particle temperature and velocity, but injection location and oxidizer dilution mainly affect particle temperature, not velocity.

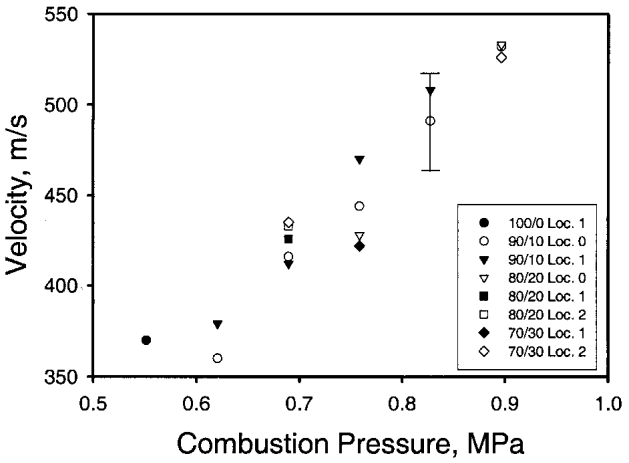

Fig. 3 Relation between particle velocity and combustion chamber pressure

Measured particle temperature T_p is plotted against particle velocity V_p in Fig. 4 for various oxidizer dilution levels and nozzle particle-injection locations. Independent variations in velocity and temperature are possible in a range primarily below the melting point of the material. Through careful selection of torch running conditions, the plot shows how several horizontal and vertical "cuts" can be made through the available range of test conditions, holding either particle velocity or temperature approximately constant. Observation of coating micrographs along with quantitative measurements can then be used to ascertain the independent effects of particle velocity and temperature.

While it is clear that independence was achieved over a significant range, there is a conspicuous absence of data for low-temperature particles between 450 and 550 m/s. This region is devoid of data because oxidizer gas mixtures containing more than 30% nitrogen diluent by weight inhibit ignition in the current HVOF combustion chamber. Such mixtures were predicted

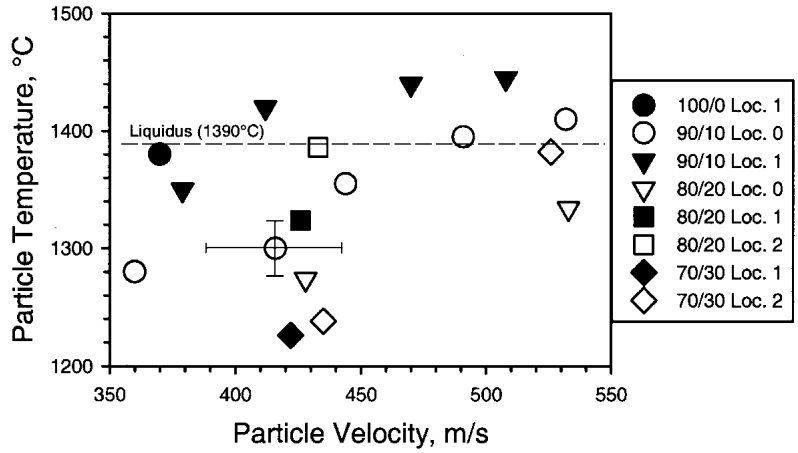

Fig. 4 Matrix of average particle temperatures and velocities

to provide low-temperature, high-velocity particles. As it turns out, however, the most useful results of this study do not require data in that region.

Note that, in Fig. 4, data points lying on the liquidus line (1390 °C for 316 stainless steel) are not necessarily fully molten, since their external temperature is sensed by pyrometry, and they are not necessarily temperature-isotropic.

The effects of independent changes in particle velocity and temperature are now explored in turn.

4.5 Temperature Effect on Coating Morphology

When particle temperature increases, spray particles simultaneously become more ductile and more prone to oxidation. Unfortunately, no quantitative data on the ductility of stainless steel at elevated temperatures was found. It can be said in general, however, that properties such as the ultimate tensile strength and hardness decrease as the material temperature nears the melting point, suggesting that ductility increases over this same range. Thus, as particle temperature T_p rises, the particle splats offer less resistance to deformation and are generally more flattened for a given V_p. Particle oxidation, while an exponential function of temperature, remains small until a significant fraction of the spray particles have temperatures above the melting point of the material.

To demonstrate the effect of particle temperature on coating morphology at constant particle velocity, groups of coating metallographs are now shown. The first group shows coatings at the low-velocity end of the present HVOF range, approximately 370 m/s (Fig. 5). Note that while, for brevity, only single micrographs are shown for each condition, the analysis is based on the examination of three micrographs taken at different coating locations for each of the seventeen conditions in the test matrix.

It is apparent from these three micrographs that the coatings are formed almost entirely of particles that remain unmelted in flight. The present stainless steel powder was gas-atomized and rapidly quenched, causing a fine internal particle grain structure. If the particles remain solid in flight, this fine grain structure is still visible after the coating is etched [indicated by a white arrow in Fig. 5(c), for example]. Moreover, the largest splats in the coating are deformed little from their original spherical shape.

Another set of coating micrographs with particle velocities V_p centered around 420 m/s, slightly below the middle of our present velocity range, is shown in Fig. 6. Coatings (a) and (b) were formed of particles over 90 °C below the melting temperature. These coatings show no oxidation except on the thin splat boundaries. The splats appear to be somewhat more deformed in (b) than in (a), as should be expected with a temperature increase of 70 °C. Coating (c) has splats that are more deformed than (a) or (b), and the porosity is correspondingly lower. Oxidation is still mostly confined to the splat boundaries because only a few particles are fully molten upon impact. The additional increase in average particle temperature evidenced in coating (d), however, now reveals noticeable regions where molten, oxidized particles have contributed to the coating.

Comparing the extreme coatings, (a) and (d) in Fig. 6, it is apparent that the splats are deformed much more in the higher-temperature coating (d). While two areas of apparent porosity are seen at the top of (d), these are, in fact, artifacts of the polishing process. By contrast, porosity is scattered throughout (a). Again, noticeable coating oxidation is seen only in coating (d).

The highest-velocity coatings in which temperature was independently varied are next shown in Fig. 7. The trends here are similar to those in the coatings already illustrated. Splat deformation increases with particle temperature, and conversely, coating porosity decreases. In particular, coating porosity decreases noticeably with increased temperature once a small fraction of the particles becomes fully molten. The oxidation in coatings (a) and (b) is still confined to the splat boundaries, since there is no evidence of molten particles in either coating. Coating metallograph (c), however, has a significant fraction of molten particles. The oxidized portions of (c) display the "marble-cake" layered appearance (indicated by white arrow) that is typically associated with high-temperature coatings, where veins of oxide are visible between layers of unoxidized metal.

From the coatings shown in Fig. 5-7, it is also clear that the smallest particles are, on average, also the hottest particles, as predicted by the particle dynamics code[1] and by elementary heat transfer arguments. The evidence for this is found in the

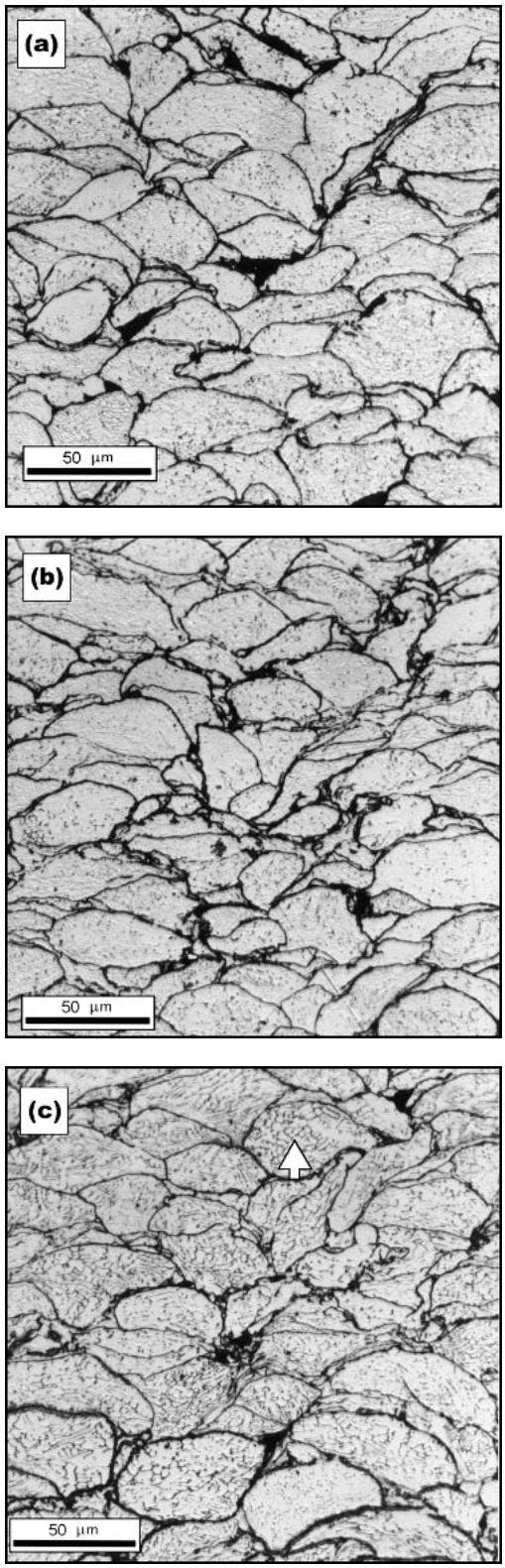

Fig. 5 Micrographs of coating cross-sections at low particle velocity V_p with variable particle temperature T_p. **(a)** 90/10, Location 0, $P_c = 0.61$ MPa, $V_p = 360$ m/s, $T_p = 1280$ °C; **(b)** 90/10, Location 1, $P_c = 0.61$ MPa, $V_p = 380$ m/s, $T_p = 1350$ °C; **(c)** 100/0, Location 0, $P_c = 0.54$ MPa, $V_p = 370$ m/s, $T_p = 1380$ °C. White arrow in Fig. 5(c) indicates fine grain structure preserved from gas-atomized powder

fully molten splats, which appear to have sizes commensurate only with the smaller particles of the powder size distribution. Oxidation is otherwise confined to the splat boundaries when particle temperatures are below the melting temperature. A small fraction of fully molten particles changes the appearance of the coating by filling in the porosity and introducing regions of significant internal oxidation. Since 1% iron oxide by weight corresponds to 6% oxide by volume,[11] a relatively small fraction of oxidized particles can impart widespread oxidation effects throughout the coating. Increasing the average particle temperature also affects the coating by softening the particles and enhancing the amount of splat deformation for a given particle velocity. The largest particles seem relatively unaffected, on the other hand, as can be noted in all the micrographs shown thus far. Overall, however, increased average temperature T_p tends to soften the particles and produce flatter splats, resulting in the observed trend toward decreased porosity with increased particle temperature.

4.6 Effect of Particle Velocity on Coating Morphology

While particle temperature affects several coating characteristics, particle velocity is mainly associated with the kinetic energy of the sprayed particles. Velocity effects are therefore manifest by the extent of splat deformation seen in the coatings, and the possibility of "impact fusion."[13,14] In these experiments, the highest average particle velocities were approximately 50% greater than the lowest average velocities. Thus, the average kinetic energy of the high-velocity particles was about double that of the low-velocity particles. This change is sufficient to discern differences among the coatings, which are shown and discussed below.

A group of low-temperature coatings where particle velocity was varied is shown in Fig. 8. While the particle temperature does increase by 50 °C from (a) to (c), the change in splat morphology is clearly most affected by the peening effect of increasing particle velocity. The splats in (c) are more deformed and flatter than those in (a) or (b). Porosity is apparent in each coating, but there appears to be little change in porosity among the coatings shown. Again, since the particles are not molten, oxidation is seen only on the splat boundaries.

A second group of coatings with higher average particle temperatures than in Fig. 8 is given in Fig. 9. Again, the splats become visibly more deformed with increasing velocity. Nevertheless, the porosity of the coatings does not appear to be decreasing as the deformation increases. [The horizontal lines seen in Fig. 9(a) are scratches due to imperfect polishing]. The large void in the same micrograph is likewise a pullout artifact of polishing. Despite measured average particle temperatures near the liquidus of 316 stainless steel, it appears that only the smallest particles were fully molten upon impact in these coatings.

The four micrographs in Fig. 10 show how the morphology of the present coatings changes when a significant fraction of the particles is molten upon impact. Comparing coatings (a) and (d), the effect of the 110 m/s increase in particle velocity between them is not obvious. Little porosity is apparent in any of these micrographs, further substantiating that particle temperatures

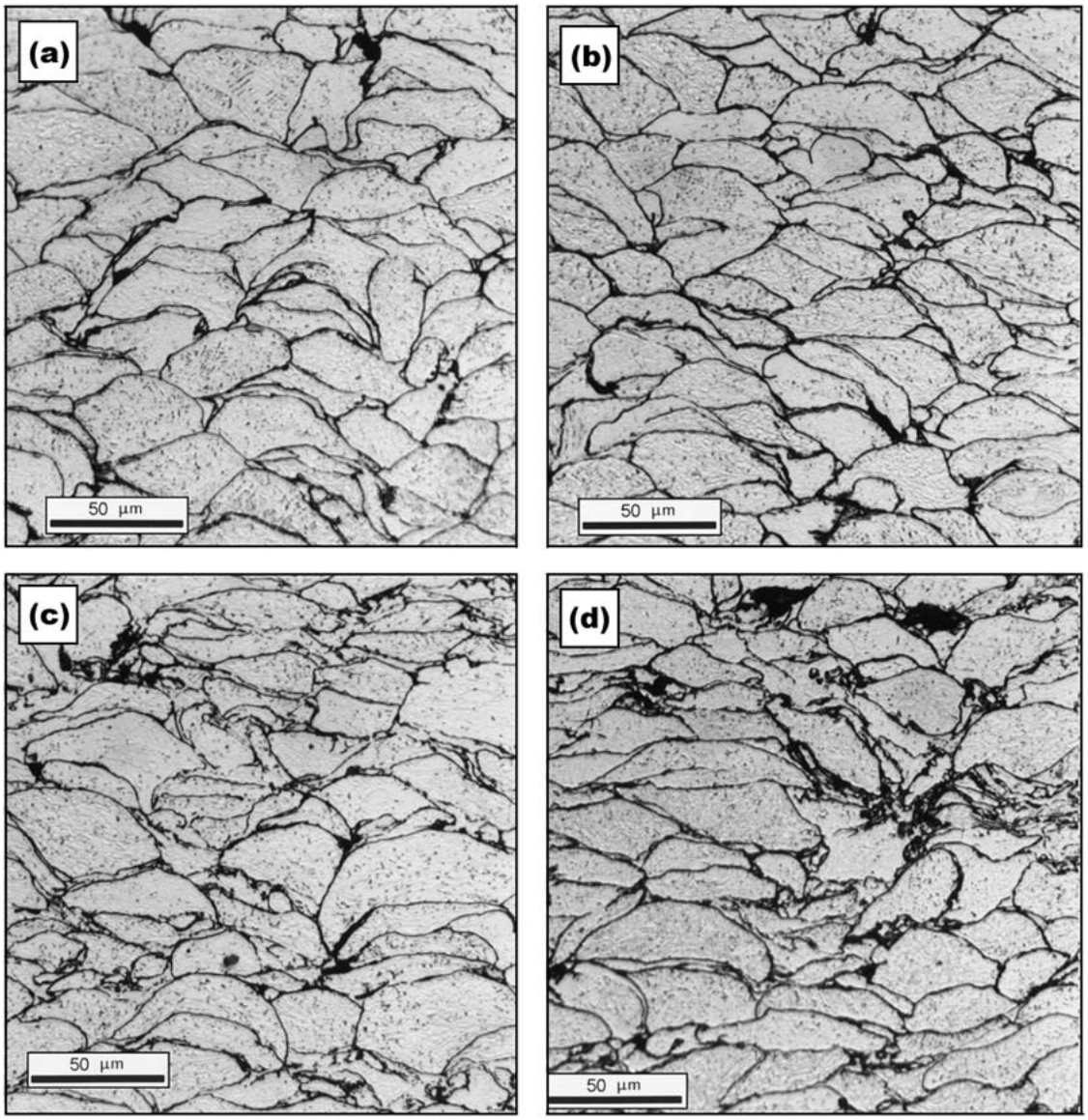

Fig. 6 Micrographs showing the effect of moderate V_p with variable T_p. **(a)** 70/30, Location 1, P_c = 0.83 MPa, V_p = 420 m/s, T_p = 1230 °C; **(b)** 90/10, Location 0, P_c = 0.69 MPa, V_p = 410 m/s, T_p = 1300 °C; **(c)** 80/20, Location 2, P_c = 0.69 MPa, V_p = 435 m/s, T_p = 1390 °C; **(d)** 90/10, Location 1, P_c = 0.69 MPa, V_p = 400 m/s, T_p = 1420 °C

near the melting temperature are required to deform particles sufficiently to produce dense coatings within the range of particle velocities attained in this experiment.

The trends seen in Fig. 8-10 are primarily those of particle deformation. The increased kinetic energy associated with high-velocity particles causes the resulting splats to deform more than their low-velocity counterparts. As expected, the softer particles associated with higher temperatures also tend to deform more than colder particles. Consequently, the higher-temperature coatings generally have less porosity.

As discussed earlier, Sturgeon and Buxton[5] note that, while limited oxidation may actually enhance coating corrosion resistance, the presence of porosity is always detrimental. From this, then, it is logical to encourage particle temperature control in a way that keeps the average T_p near the material melting point. Insofar as coating porosity nears zero when a small fraction of the spray particles is molten, coating corrosion resistance, within limits, may profit from elevated particle temperatures.

On the other hand, once a fraction of the spray particles becomes molten, the average particle velocity appears to have little effect on the morphology of the splats. Thus, while higher particle temperature simultaneously promotes splat deformation and oxidation, higher particle velocity appears to gradually increase splat deformation without undesirable side effects.

The unexpected result that a particle velocity increase promotes splat deformation but does not strongly affect coating porosity deserves further comment. The composition of 316L stainless is traditionally chosen for exceptional corrosion resistance and ability to resist creep at elevated temperatures. Nevertheless, the ductility of all metals including stainless steel must increase as the melting temperature is approached. Increasing

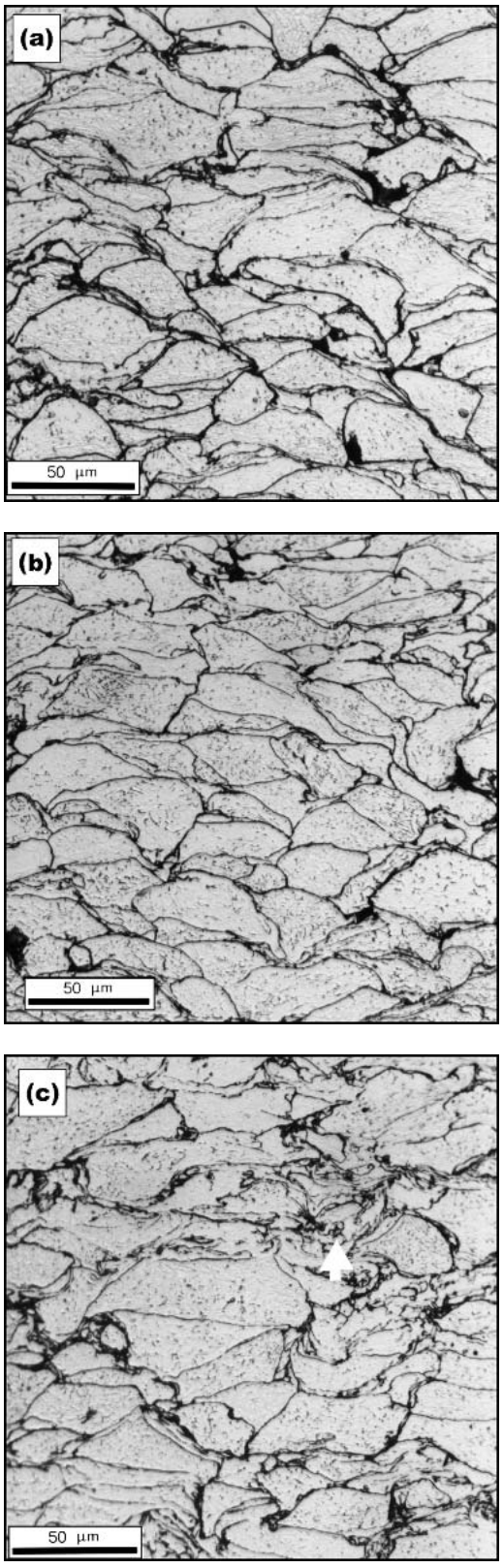

Fig. 7 Micrographs showing effects of high V_p with variable T_p. **(a)** 80/20, Location 0, P_c = 0.90 MPa, V_p = 530 m/s, T_p = 1330 °C; **(b)** 70/30, Location 2, P_c = 0.90 MPa, V_p = 530 m/s, T_p = 1380 °C; **(c)** 90/10, Location 0, P_c = 0.90 MPa, V_p = 530 m/s, T_p = 1410 °C. White arrow in Fig. 7(c) indicates oxidized layers

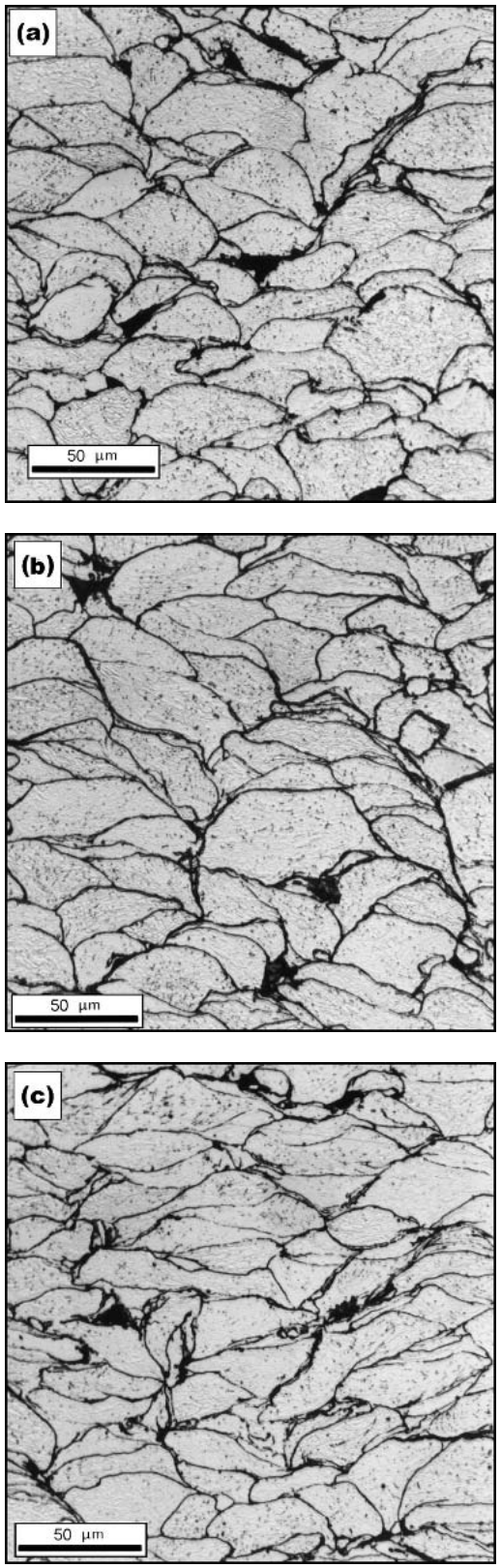

Fig. 8 Micrographs of showing effects of low particle T_p with variable V_p. **(a)** 90/10, Location 0, P_c = 0.62 MPa, V_p = 360 m/s, T_p = 1280 °C; **(b)** 90/10, Location 0, P_c = 0.69 MPa, V_p = 415 m/s, T_p = 1300 °C; **(c)** 80/20, Location 0, P_c = 0.90 MPa, V_p = 530 m/s, T_p = 1330 °C

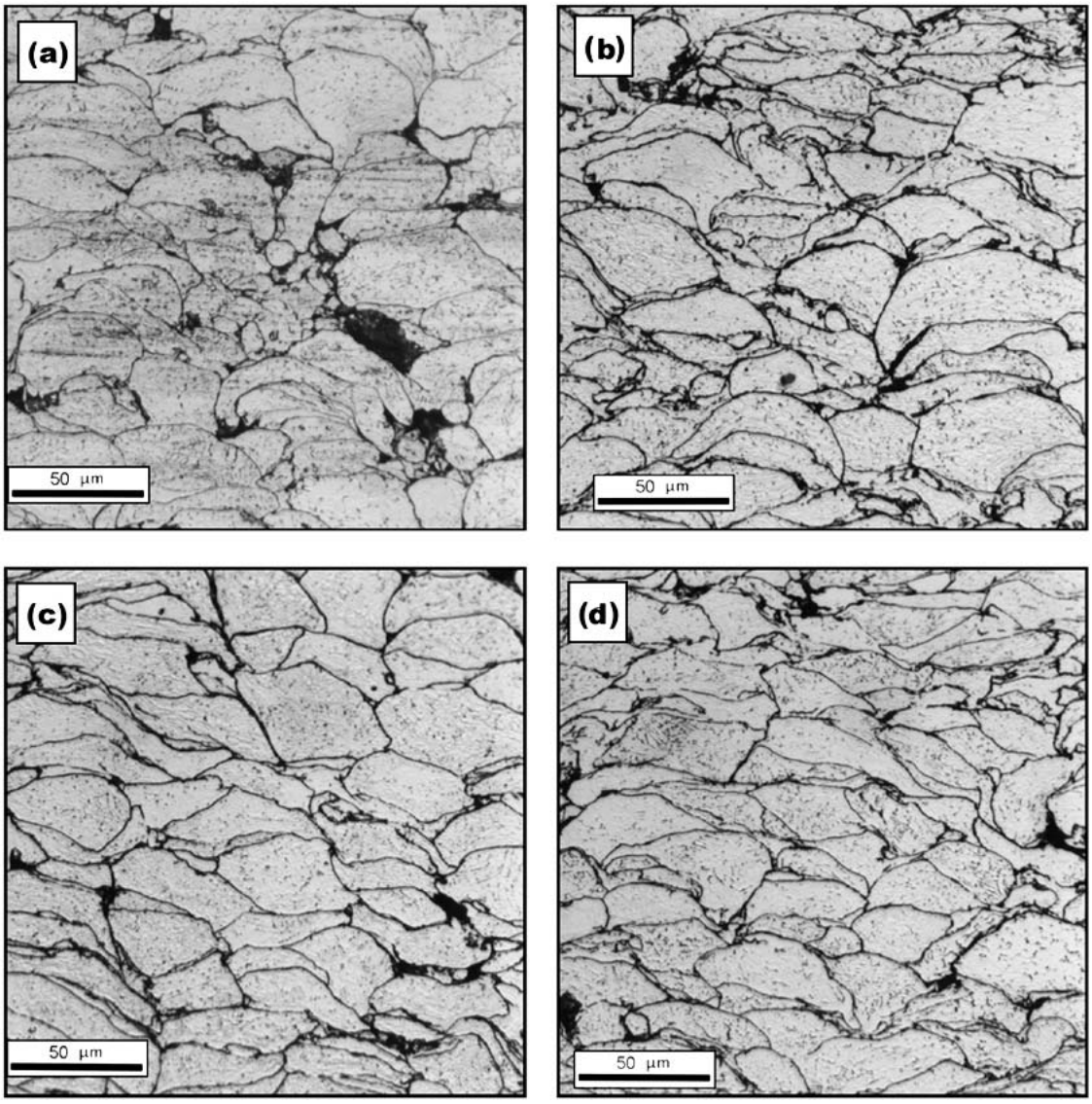

Fig. 9 Micrographs of coating cross-sections with moderate T_p and variable V_p. **(a)**100/0, Location 0, P_c = 0.55 MPa, V_p = 365 m/s, T_p = 1380 °C; **(b)** 80/20, Location 2, P_c = 0.69 MPa, V_p = 430 m/s, T_p = 1390 °C; **(c)** 90/10, Location 0, P_c = 0.83 MPa, V_p = 490 m/s, T_p = 1390 °C; **(d)** 70/30, Location 2, P_c = 0.90 MPa, V_p = 530 m/s, T_p = 1380 °C

particle velocity favors splat deformation, so why should it not also reduce porosity? A possible answer appears from further analysis of the present coatings. The spray particles are roughly spherical while in flight, but they become flattened splats upon impact. It appears from the present micrographs that porosity (excepting that caused by "pull-outs" due to the polishing process) exists only at the peripheries of the splats. Porosity is thus fundamentally an issue of insufficient splat deformation. Until particle velocities become high enough that certain oddly shaped surface cavities can be filled, fully dense coatings are not attainable from cold, hard spray particles. Thus, fully dense coatings require both sufficient particle velocity and particle ductility. Consequently, in-flight particle temperature becomes the key variable since it determines splat ductility. High particle velocity is nonetheless desirable, as analysis of the micrographs reveals, and one should seek the highest velocities attainable while simultaneously keeping particle temperatures near the material melting point.

The micrograph shown in Fig. 11 represents those coatings formed of a large fraction of fully molten particles. Unlike the coatings shown previously, where only the smallest particles were molten upon impact, here only the largest particles remain unmelted. The layered "marble-cake" appearance noted earlier is prevalent here throughout the coating. Further, it is clear that the original grain structure of the spray particles is now visible only in the largest (unmelted) splats, but has disappeared for all smaller, molten splats. The coating is substantially oxidized, but its porosity is exceptionally low; in fact, no pores are visible at all. Clearly then, higher-temperature coatings have reduced porosity even after the spray particles are predominantly molten upon impact. The tradeoff between coating oxidation and porosity is apparent here.

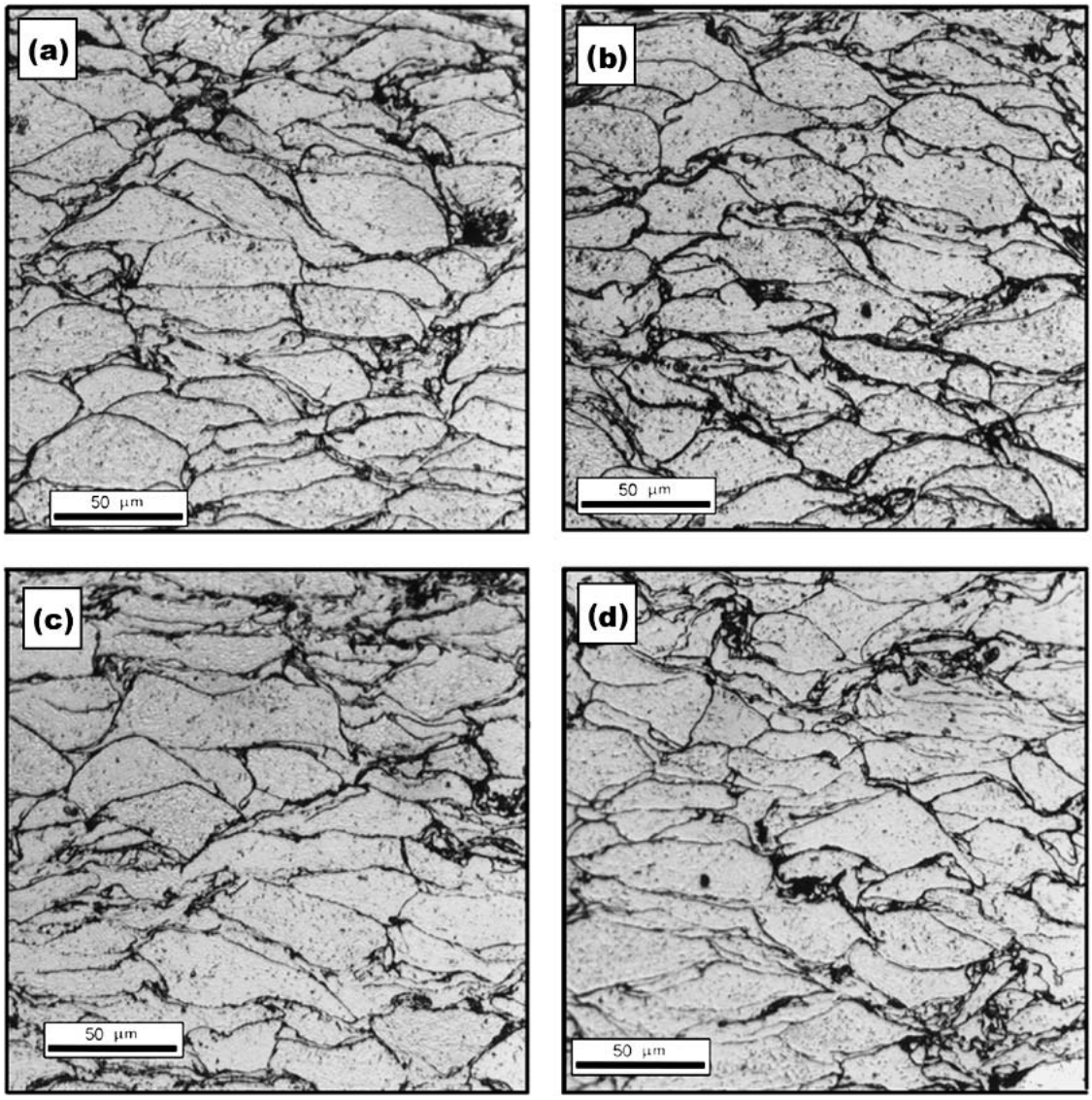

Fig. 10 Micrographs of coating cross-sections with high T_p and variable V_p **(a)** 90/10, Location 1, P_c = 0.69 MPa, V_p = 410 m/s, T_p = 1420 °C; **(b)** 90/10, Location 1, P_c = 0.76 MPa, V_p = 470 m/s, T_p = 1440 °C; **(c)** 90/10, Location 1, P_c = 0.83 MPa, V_p = 510 m/s, T_p = 1450 °C; **(d)** 90/10, Location 0, P_c = 0.90 MPa, V_p = 530 m/s, T_p = 1410 °C

4.7 Trends in Coating Porosity

The effects of particle velocity and temperature on coating porosity are next discussed quantitatively. It has been demonstrated through the micrographs that increased temperature softens spray particles, and that these particles then deform more readily at a fixed kinetic energy level. Once some particles become molten, coating porosity quickly tends toward zero. Increased velocity also causes particles to deform more, but it does not have such an obvious effect on coating porosity.

The technique described earlier to measure coating porosity is not a perfect quantitative measure. This is due to pullouts of some splats in the coating cross-sections during the polishing process. Since it is generally difficult to determine whether a void in a metallograph is due to the polishing process or to a true pore in the coating, the coating porosity was measured in two different ways: in Fig. 12, the porosity was estimated by including all of the voids seen in all metallograms, even those that are clearly pull-outs. Conversely, Fig. 13 shows the results of the measurement when all possible pullout voids are excluded. The true porosity level in each of the coatings lies somewhere between these two measurements. Nevertheless, they are identical in trend though different in degree. Thus the combination of both indicators provides at least a semiquantitative basis for coating porosity comparisons.

Inspection of all the current metallographs further reveals that the lowest-temperature coatings tend to have many more pullouts than their hotter counterparts, which is also seen in the comparison of the previous two plots. This suggests that the splat bonding among colder particles is inferior to that among hotter particles. Dobler et al., among others, have previously made this observation.[4]

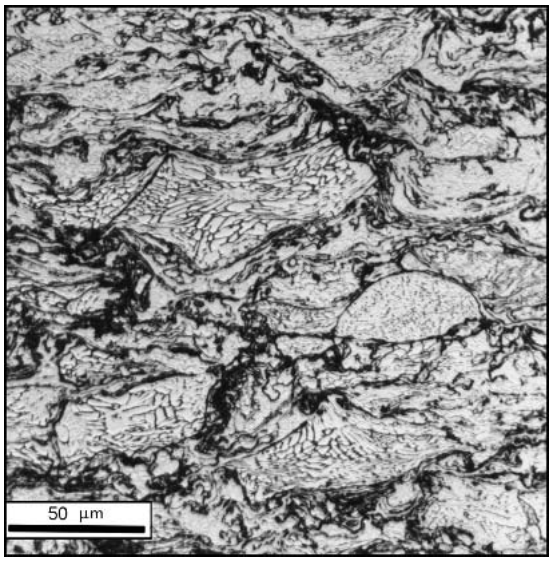

Fig. 11 Micrograph of a coating formed of high-temperature splats. 100/0, Location 1, P_c = 0.93 MPa, T_p = 1520 °C

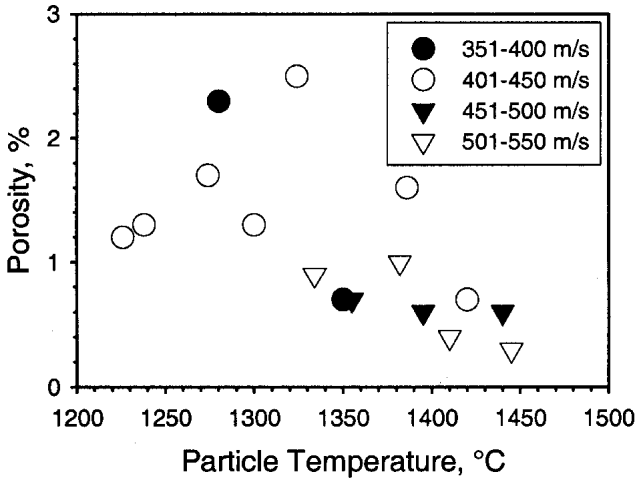

Fig. 12 Porosity measurement including pullouts

In Fig. 13, the slowest-, coldest-particle coatings have porosity levels of approximately 0.6%, while the fastest, hottest coatings have porosity levels of only about 0.1%. This trend further demonstrates that particle temperature control is a critical factor in creating dense coatings. Whereas it was previously thought that low-temperature, high-velocity particles can create highly-dense coatings, e.g., in coatings formed by the cold-spray process,[9,11,13,14] these experiments show that even high-velocity HVOF-sprayed particles of 316L stainless steel yield dense coatings only when the average particle temperature is near (or above) the material melting temperature. Supporting this further is present evidence that even hot, low-velocity particles possess sufficient kinetic energy to create low-porosity coatings. Thus, while high particle velocities are clearly desirable, it is evident that without sufficient particle heating, coating density and quality both suffer.

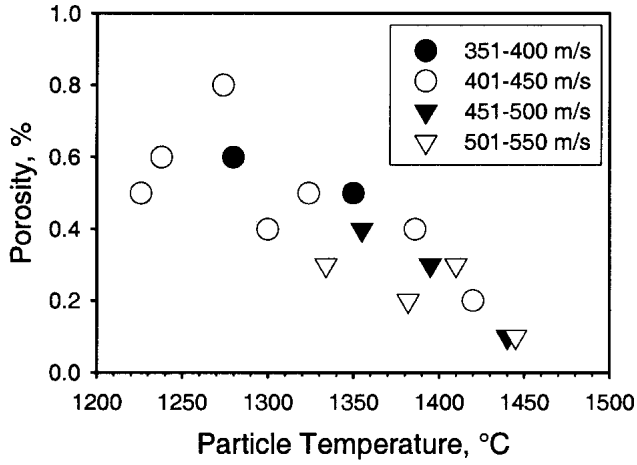

Fig. 13 Porosity measurement excluding all pores that could be pullouts

4.8 Trends in Coating Oxidation

The micrographs shown earlier demonstrate that coating oxidation levels in these experiments are related to particle temperature alone, as expected. The plot given in Fig. 14 shows quantitatively how oxidation increases with particle temperature. There is a marked "knee" in the curve near the melting point of stainless steel, where coating oxidation begins a rapid increase with further temperature rise. This increase in oxygen content corresponds well with the qualitative appearance of oxidized regions seen in the micrographs. On the other hand, for particle temperatures within 180 °C below the liquidus, the coating oxide level is relatively constant at about 0.25%.

Thus, two independent indicators show that stainless steel coating oxidation increases markedly only when spray particle temperature exceeds the melting point of the material. Note that the unsprayed powder contains about 0.023% oxygen by weight, which is about one-tenth of that found in even the lower-temperature coatings. Since the oxidation level changes only slowly with temperature before molten particles appear, there is thus little advantage in reducing particle temperature very far below the material melting point. Nevertheless, the rapid increase in oxidation that occurs above the melting point demonstrates the desirability of keeping particle temperatures at or below the melting temperature if oxidation is to be minimized. Again, the results of Sturgeon and Buxton[5] and Dobler et al.[4] suggest that some small level of oxidation in coatings is beneficial, though this conclusion may have been influenced by their inability to separate particle velocity and temperature in their experiments.

4.9 Effect on Deposition Efficiency

In light of the expense of spray powder, deposition efficiency must be considered in addition to coating oxidation and porosity. In a small study, we examined how changes in the particle temperature affect the deposition efficiency. Figure 15 shows the results. (These measurements are preliminary; thus the error in the deposition efficiency is estimated to be at least the size of the data points shown in the plot.)

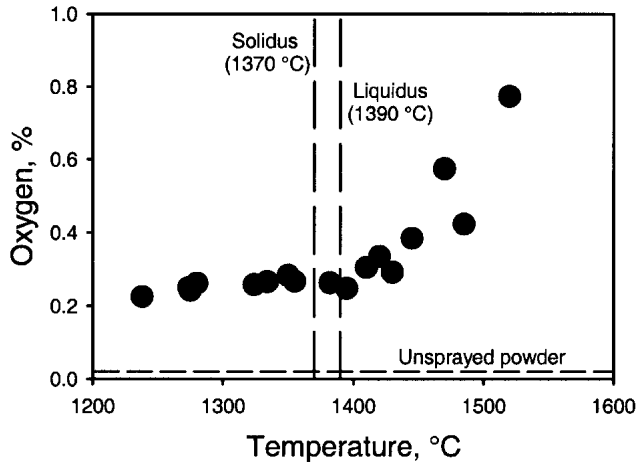

Fig. 14 Relation between coating oxygen content by weight and average particle temperature

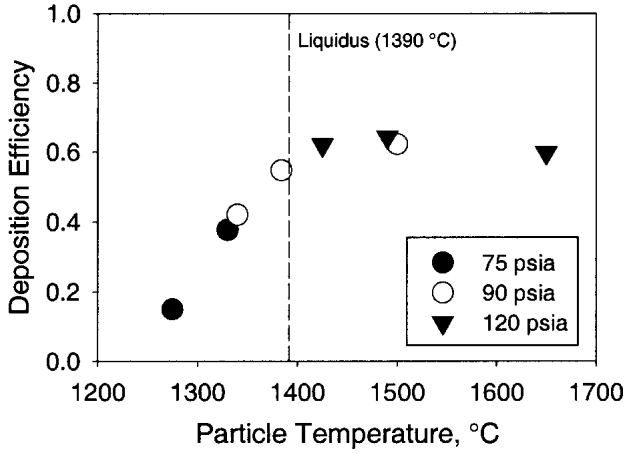

Fig. 15 Effect of particle temperature on deposition efficiency

The effect of temperature on the fraction of particles deposited is strong below the material melting point. Consistent with the results already presented, the increased deposition efficiency in this temperature range is certainly a result of increasing particle ductility with increasing temperature. However, after the average particle temperature exceeds the material melting point, the deposition efficiency becomes approximately constant with temperature. The 15% deposition efficiency seen for the lowest-temperature coating represents poor usage of the expensive spray powder. On the other hand, the deposition efficiency for T_p near or above the melting point, approximately 60%, represents a four-fold improvement.

5. Conclusions

In this study, the independent effects of spray particle velocity and temperature on HVOF stainless steel splat morphology, coating porosity, and coating oxidation were assessed. Prior to these experiments, we expected that high-velocity, low-temperature particles would produce the highest-quality coatings having both low oxidation and low porosity, and benefiting from impact fusion.[13,14] This expectation also arose in part from our previous measurements[6] in which the separation of velocity and temperature was restricted to a small range. Furthermore, the advantages of the cold-spray process are largely based such assumptions.

Present results show that a range of particle velocities and temperatures clearly exists within which process efficiency and coating characteristics may be optimized for a given spray material. It appears that a certain level of oxidation is unavoidable in the spray process and that this level is relatively unaffected by particle temperature until at least some particles become molten upon impact. It is interesting that this baseline level of oxygen found in the present coatings, approximately 0.25% by mass, is also unaffected by widely-varying combustion gas mixtures that included as much as 30% nitrogen diluent by mass. Previous experiments by Hackett using a nitrogen gas shroud showed that particle oxidation can be kept constant across a wide range of spraying conditions, whereas unshrouded molten particles become highly oxidized by atmospheric oxygen entrainment into the HVOF spray.[1] This suggests that the oxygen contained in coatings formed of unmelted particles is an artifact of the time the particles spend within the HVOF torch.[15,16]

The present measurements of coating porosity show that even high-velocity particles have insufficient kinetic energy to deform to an extent where porosity is below 0.2% if those particles are much below the material melting temperature. Since increased temperature softens the particles, however, relatively low-velocity particles can yield highly dense coatings given sufficient particle temperature. Since particle deformation and coating density increase with temperature, especially when the average particle temperature nears the material melting point, it appears that the ideal spray particle temperatures are in the vicinity of the liquidus of the material. Voggenreiter et al. already reached this conclusion, though by different experimental methods than those used here and without either T_p or V_p measurements.[2]

By contrast, particle velocity appears to play a less-significant role in HVOF-sprayed coatings than had previously been thought. While particles deform more as their kinetic energy prior to impact increases, low-temperature particles still do not deform sufficiently to produce coatings with porosity below 0.1%. Still, all the present evidence indicates that higher particle velocity, when particle temperature can be independently controlled, is desirable for high-quality coatings.

Considering coating oxidation, it is clear that particle temperatures should not far exceed the material melting temperature. The oxidation advantages of having cold particles, however, are few, since the coating oxidation level diminishes very slowly with particle temperature T_p when T_p is below the melting point. For corrosion-resistant coatings, there is evidence that a low level of oxidation in the coating actually improves corrosion resistance.

Deposition efficiency adds an economic incentive to the quality-based reasons for HVOF spraying near the melting point. Spraying much below the melting point results in poor deposition efficiency, while deposition efficiency is notably improved with spray temperatures near or above the melting point.

Full process diagnostics for commercial HVOF spraying are very expensive. This research suggests, however, that full diagnostics may not be needed, but particle temperature measurement and feedback control appear to be essential in obtaining the best-quality anti-corrosion coatings.

Nothing presented here supports HVOF spray processes that are much colder than the melting point of the sprayed material. From this, then, one can conclude that ideal HVOF spray conditions for creating dense, low-oxide coatings include high particle velocities and especially particle temperatures near or slightly above the melting point of the material. "Cold spray" violates this rule but is in a category of its own, with high particle velocities but much colder particle temperatures than those considered in this study.

Acknowledgments

The authors thank J.D. Miller and Lori Dreibelbis for their assistance throughout the course of these investigations. This research was supported by the DOE-BES (Basic Energy Science) Materials and Engineering Program and administered by Dr. Robert E. Price.

References

1. C.M. Hackett: "The Gas Dynamics of High-Velocity Oxy-Fuel Thermal Sprays," Ph.D. Thesis, Dept. of Mechanical and Nuclear Engineering, UMI Order Number 9628094, Pennsylvania State University, 1996.
2. H.F. Voggenreiter, S. Huber, S. Beyer, and H-J. Spies: "Influence of Particle Velocity and Molten Phase on the Chemical and Mechanical Properties of HVOF-Sprayed Structural Coatings of Alloy 316L" in *Advances in Thermal Spray Science and Technology*, C.C. Berndt and S. Sampath, ed., ASM International, Materials Park, OH, 1995. pp. 303-08.
3. H.F. Voggenreiter, H. Huber, H-J. Spies, and H. Baum: "HVOF-Sprayed Alloy In718 — The Influence of Process Parameters on the Microstructure and Mechanical Properties" in *Forum for Scientific and Technological Advances*, C.C. Berndt, ed., ASM International, Materials Park, OH, 1997.
4. K.H. Dobler, H. Kreye, and R. Schwetzke: "Oxidation of Stainless Steel in the High Velocity Oxy-Fuel Process," *J. Therm. Spray Technol.,* 2000, *9*(3), pp. 407-13.
5. A.J. Sturgeon and D.C. Buxton: "The Electrochemical Corrosion Behavior of HVOF Sprayed Coatings" in *Thermal Spray Surface Engineering via Applied Research.* C.C. Berndt, ed., ASM International, Materials Park, OH, 2000, pp. 1011-15.
6. T.C. Hanson, C.M. Hackett, and G.S. Settles: "Independent Control of HVOF Particle Velocity and Temperature," *J. Therm. Spray Technol.,* 2002, *11*(1), pp. 75-85.
7. A.P. Alkhimov, V.F. Kosarev, and A.N. Papyrin: "A Method of 'Cold' Gas-Dynamic Deposition," *Dokl. Akad. Nauk SSSR*, 1990, *315,* pp. 1062-65.
8. R.C. McCune, W.T. Donlon, O.O. Popoola, and E.L.Cartwright: "Characterization of Copper Layers Produced by Cold Gas-Dynamic Spraying," *J. Therm. Spray Technol.,* 2000, *9*(1), pp. 73-82.
9. R.C. Dykhuizen and M.F. Smith: "Gas Dynamic Principles of Cold Spray," *J. Therm. Spray Technol.,* 1998, *7*(2), pp. 205-12.
10. E.E. Underwood: *Quantitative Stereology*. Addison-Wesley, Reading, MA, 1970.
11. R.C. McCune, W.T. Donlon, E.L. Cartwright, A.N. Papyrin, E.F. Rybicki, and J.R. Shadley: "Characterization of Copper and Steel Coatings Made by the Cold Gas-Dynamic Spray Method" in *Thermal Spray: Practical Solutions for Engineering Problems*, C.C. Berndt, ed., ASM International, Materials Park, OH, 1996, pp. 397-403.
12. T.C. Hanson: "Independent Control of Particle Velocity and Temperature in the High-Velocity Oxy-Fuel Spray Process," Masters Thesis, Department of Mechanical and Nuclear Engineering, Pennsylvania State University, State College, PA, 2001.
13. J.A. Browning: "Hypervelocity Impact Fusion — A Technical Note," *J. Therm. Spray. Technol,* 1992, *1*(4), pp. 289-92.
14. J.A. Browning: "HVIF/Cold Spray?," *Spraytime*, 4th Quarter 2001, p. 7.
15. M.F. Smith, R.C. Dykhuizen, and R.A. Neiser: "Oxidation in HVOF-Sprayed Steel" in *Thermal Spray: A United Forum,* C.C. Berndt, ed., ASM International, Materials Park, OH, 1997, pp. 885-93.
16. R.A. Neiser, M.F. Smith, and R.C. Dykhuizen: "Oxidation in Wire HVOF-Sprayed Steel," *J. Therm. Spray Technol. 7*(4), 1998, pp. 537-45.